

NANOPARTICLES

https://doi.org/10.1070/QEL16789

Synthesis of silver nanospheroids in silver-containing nanoporous glass under the effect of nanosecond laser pulses

A.I. Sidorov, T.V. Antropova

Abstract. **Experimental evidence is presented that nanosecond laser irradiation of nanoporous silicate glass containing subnanometre Ag_n molecular silver clusters leads to the formation of spheroidal silver nanoparticles in the glass pores. Their shape has been confirmed by numerical simulation and electronic-microscopic images. The main processes induced by laser irradiation are local heating and the photoionisation and photofragmentation of the molecular silver clusters, followed by the aggregation of the fragments of the molecular clusters into nanoparticles.**

Keywords: *laser irradiation, silver, molecular cluster, nanoparticle, plasmon resonance, nanoporous glass.*

1. Introduction

Composite materials containing metal nanoparticles in which plasmon resonance is possible [1, 2] are widely used in chemical and biological sensors [3–5], nonlinear optical devices [6, 7] and nanoplasmonics [8, 9]. Laser irradiation of metal-containing composites makes it possible to modify their structure and the geometry and size of metallic nanoparticles and, therefore, to control the optical properties of the composites. As shown earlier [10–12], pulsed laser irradiation of solid or liquid composites containing metallic nanoparticles leads to photodestruction of the nanoparticles and a decrease in their size or to their transformation into subnanometre molecular clusters. Conversely, laser irradiation and subsequent heat treatment of glass containing silver ions lead to the formation of silver nanoparticles in the glass [13, 14].

Silicate nanoporous glasses (NPGs) containing interconnecting pores [15–17] are convenient matrices for the synthesis of nanoparticles. Each glass pore can be thought of as a nanoreactor in which one can run multistep chemical reactions and modify particular properties of the synthesised nanoparticles and nanostructures using external influences (irradiation, heat treatment and others). Producing metallic or semiconducting nanoparticles or nanostructures in NPG, one can prepare novel functional materials for electronic, optoelectronic, photonic and sensing applications. Heating an NPG-based composite to 900–950 °C causes the glass pores to collapse, and the NPG converts into monolithic quartzoid glass containing inclusions in the form of nanoparticles.

As shown by Burchianti et al. [18], laser irradiation of rubidium-containing NPG leads to either the formation or photodestruction of rubidium nanoparticles (depending on laser irradiation conditions). Marmugi et al. [19] showed that laser irradiation of potassium-containing glass led to the formation of spheroidal potassium nanoparticles. They proposed using the observed effects for optical information recording. The effect of laser irradiation on silver halide-containing NPGs has been the subject of several studies [20–22]. CW laser irradiation (at λ = 1.07 μm and 355 nm) produces colloidal silver nanoparticles in such NPGs. Nanosecond laser pulses (λ = 1.06 μm) incident on NPGs containing silver and copper halides were observed to modify the zone under irradiation due to the formation of metallic nanoparticles.

In this paper, we examine effects resulting from the irradiation of silver-containing NPGs with nanosecond laser pulses, analyse the influence of such irradiation on the optical properties of the NPGs and discuss the mechanisms responsible for the formation of silver nanoparticles.

2. Experimental

In our experiments, we used silicate NPGs containing interconnecting pores 3.5 nm in average size. The glasses were prepared at the I.V. Grebenshchikov Institute of Silicate Chemistry, Russian Academy of Sciences. Their porosity was 20% to 25%. It is worth noting that pores 3.5 nm in size contain secondary silica nanoparticles, which determine the volume of the free space in the pores. SiO_2 accounts for more than 95% of the NPG network. Electron-microscopic images of the NPGs were presented previously [23]. Glass samples had the form of polished plates 10 × 10 × 1 mm in dimensions. The glass pores were filled with an aqueous silver nitrate solution (0.025 : 1) by immersing the NPGs in the solution for 3 h. Next, the samples were dried in the dark for 10 h and then illuminated with a mercury lamp for 20 min at room temperature. As a result of silver nitrate photolysis, the initially colourless samples turned dark grey. The gaseous photolysis products (nitrogen oxides) were removed from the pores in a natural way.

The glasses were irradiated by frequency-doubled (λ = 532 nm) LS-2131M multimode Nd : YAG laser (Lotis TII, Belarus) pulses. The laser pulse duration was 9 ns, the pulse repetition rate was 10 Hz, and the pulse energy was 75 mJ. The laser fluence was determined by the number of laser

A.I. Sidorov St. Petersburg National Research University of Information Technologies, Mechanics and Optics, Kronverkskii prosp. 49, 197101 St. Petersburg, Russia;
e-mail: ai.sido@yandex.ru, sidorov@oi.ifmo.ru;
T.V. Antropova I.V. Grebenshchikov Institute of Silicate Chemistry, Russian Academy of Sciences, nab. Admirala Makarova 2, 199034 St. Petersburg, Russia

Received 27 July 2018; revision received 25 August 2018
Kvantovaya Elektronika **48** (10) 962–966 (2018)
Translated by O.M. Tsarev

pulses, N. The average laser pulse energy density on the sample surface was 2.9 J cm^{-2}. The irradiated zone diameter on the sample surface was 1.4 mm. The samples were irradiated at room temperature in air. Preliminary experiments showed that energy densities from 3 to 3.5 J cm^{-2} caused no disintegration of or structural changes in the NPGs. The reason for this is that the network of the NPGs consists of SiO_2, which has a high optical damage threshold.

Optical density spectra were measured on a Lambda 650 spectrophotometer (PerkinElmer, USA), and Raman spectra, on an inVia Raman microscope (Renishaw, UK). All spectroscopic measurements were made at room temperature. Electron-microscopic images of silver nanoparticles in the NPGs were obtained on an EM-160 transmission electron microscope.

3. Experimental results

Figure 1a is a transmitted light photograph of an irradiated zone on silver-containing NPG. It is seen that laser irradiation causes a significant change in the colour of the NPG: from dark grey to yellow. In the spectral range 550–600 nm, the transmittance of the central part of the irradiated zone is increased twofold, with a dark peripheral part of the irradiated zone.

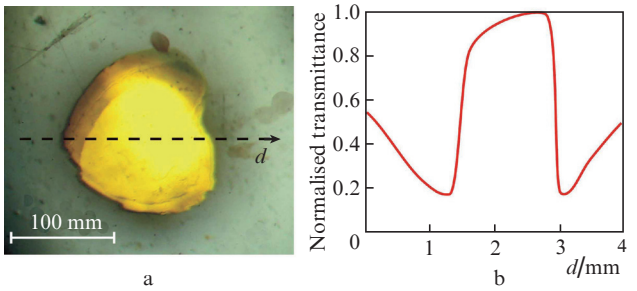

Figure 1. (Colour online) (a) Transmitted light photograph of an irradiated zone on silver-containing NPG and (b) normalised transmittance profile across the irradiated zone in the spectral range 550–600 nm; N = 600 pulses.

Figure 2 shows optical density spectra of the NPG before and after UV irradiation with the mercury lamp and after laser irradiation to various fluences. It is seen that the mercury lamp irradiation leads to a uniform increase in optical density in the spectral range 250–700 nm, with a slight maximum at λ = 350 nm. Comparison with previously reported data [24–28] leads us to conclude that a major contribution to absorption in this case is made by subnanometre Ag_n (n = 2–15) molecular silver clusters. Absorption in the short-wavelength part of the spectrum is due to the presence of Ag_2 and Ag_4 molecular clusters, and longer wavelength absorption is due to Ag_3 and Ag_n ($n \geqslant 5$) molecular clusters. The formation of molecular silver clusters in the NPG is the result of $AgNO_3$ photolysis under the effect of the UV radiation from the mercury lamp. Absorption can also be contributed by silver oxide, Ag_2O.

Pulsed laser irradiation produces a strong absorption band in the range 320–500 nm in the optical density spectrum. The band has a flat top and consists of a few absorption bands. Absorption bands of such shape are typical of absorption in the plasmon resonance region of nonspherical metallic

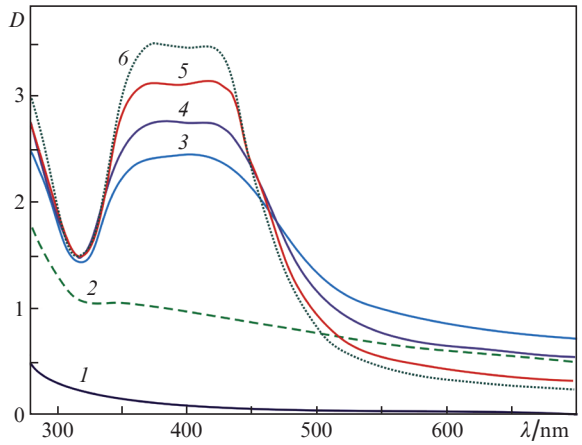

Figure 2. Optical density (D) spectra of silver-containing NPG (*1*) before UV irradiation, (*2*) after UV irradiation and (*3–6*) after laser irradiation; N = (*3*) 50, (*4*) 350, (*5*) 450 and (*6*) 620 pulses.

nanoparticles [1, 2] – silver nanoparticles in our case. The intensity of the absorption band rises with increasing laser fluence. It is seen in Fig. 2 that the increase in absorption in the spectral range 350–500 nm is accompanied by a decrease in absorption at $\lambda > 480$ nm. Figure 3 shows the optical density at λ = 400 and 550 nm as a function of laser fluence. With increasing laser fluence, the optical density at λ = 400 nm rises by a factor of 3.5. This is due to the increase in the concentration and size of silver nanoparticles. However, since the average pore size in the NPG does not exceed 3.5 nm, the size of the silver nanoparticles also cannot exceed this value. With increasing laser fluence, the optical density at λ = 550 nm first increases twofold and then drops by a factor of 4 relative to the initial optical density.

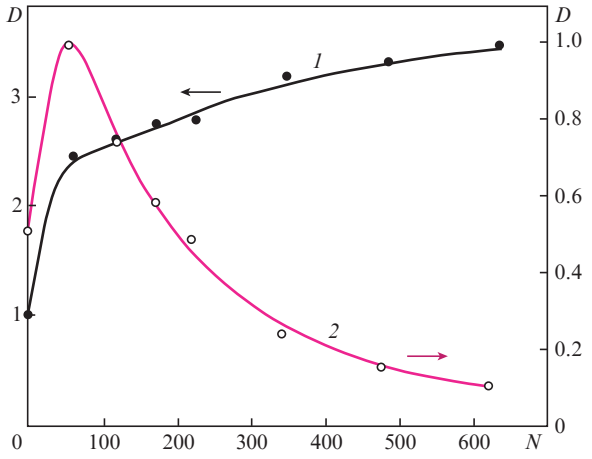

Figure 3. Optical density D at λ = (*1*) 400 and (*2*) 550 nm as a function of laser fluence.

Consider the shape of the absorption band of the silver nanoparticles in the plasmon resonance region (Fig. 2). Spherical metallic nanoparticles less than 20 nm in diameter are known to have one, symmetric and narrow, absorption band in the plasmon resonance region, with one maximum [1, 2]. The present experimental spectra differ significantly in shape from the absorption spectrum of spherical silver

nanoparticles in the plasmon resonance region. The experimental spectrum in Fig. 2 can be represented as a combination of two Gaussian absorption bands [Fig. 4, curves (*2*), (*3*)]. Such a spectrum is typical of metallic nanospheroids with axes $a = b \neq c$. In our case, the two absorption bands correspond to electron plasma oscillations along the major and minor nanospheroid axes. Since the average size of the nanoparticles does not exceed 3.5 nm, the quasi-static dipole approximation [29] can be used for numerical simulation of their optical properties. In this approximation, the absorption cross section σ_a of a nanoellipsoid can be represented in the following form [1, 2, 29]:

$$\sigma_a = k\mathrm{Im}\,\delta,$$

where δ is the polarisability of the nanoparticle and $k = 2\pi/\lambda$.

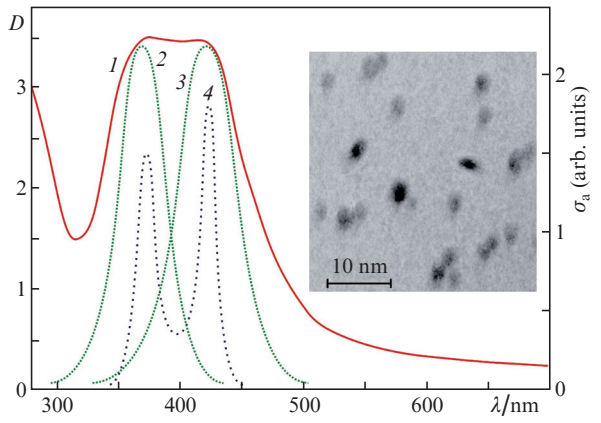

Figure 4. (*1*) Experimental absorption spectrum of the silver-containing NPG at $N = 620$ laser pulses, (*2*, *3*) decomposition of the experimental spectrum into Gaussians and (*4*) calculated absorption cross section σ_a of a silver nanospheroid with an axial ratio $a:c = 1:1.3$ in the glass. Inset: electron-microscopic image of silver nanoparticles in the NPG.

The polarisability components of a nanoellipsoid with a, b and c axes along the three coordinates ($i = 1, 2, 3$) can be represented in the form [29]

$$\delta_i = 4abc\frac{\varepsilon_p - \varepsilon_h}{3\varepsilon_h + 3L_i(\varepsilon_p - \varepsilon_h)},$$

$$L_i = \frac{abc}{2}\int_0^\infty \frac{\mathrm{d}x}{(z_i^2 + x)\sqrt{(a^2 + x)(b^2 + x)(c^2 + x)}},\ z_i = \begin{pmatrix} a \\ b \\ c \end{pmatrix}.$$

Here, ε_p and ε_h are the dielectric permittivities of the nanoparticle material and ambient medium, respectively, and L_i is the depolarisation factor for the three coordinates. Since the nanospheroids are oriented at random in the NPG, their absorption cross sections should be averaged over the three coordinates. In numerical simulation, we used the dispersion of optical constants of silver from Irani et al. [30] and $a = 3.5$ nm. It is seen in Fig. 4 that, at an axial ratio $a:c = 1:1.3$, the calculated spectral dependence of the absorption cross section for a nanospheroid [curve (*4*)] correlates well with the experimental absorption spectrum [curve (*1*)]. The broadening of the experimental spectrum compared to the calculated one is due to the scatter in the geometric shape of the actual silver nanoparticles in the NPG. Further evidence for the spheroidal shape of the silver nanoparticles is provided by the electron-microscopic image of the irradiated zone on the NPG surface in the inset in Fig. 4. It is seen in this micrograph that the nanoparticles have the shape of oblong spheroids with a characteristic size between 3 and 5 nm.

The fact that laser irradiation produces not spherical but spheroidal nanoparticles is easy to explain. The pores in the NPG are not spherical but have the form of extended channels. Therefore, the transverse growth of nanoparticles is limited by the pore walls and, accordingly, the preferential growth direction is along the channel axis.

Additional information about the processes involved in the formation of nanoparticles can be gained from the Raman spectra presented in Fig. 5. The Raman spectrum of the silver-free NPG has the form of a broad band centred near 2000 cm^{-1} [Fig. 5, spectrum (*1*)]. It is known that, under normal conditions, NPG contains monolayers of physisorbed and chemisorbed water [31]. Thus, the band in question is attributable to a $\nu_2 + L_2$ combination of vibrational modes of water molecules [32]. This band, with different intensities, is also present in the other spectra in Fig. 5. The main OH stretching bands lie in the frequency range 3000–3700 cm^{-1} [32–34] and are not shown in Fig. 5. The origin of the weak and broad band centred at 500 cm^{-1} has not been identified. After the formation of molecular silver clusters in the NPG, its Raman spectrum showed five additional bands, at 160, 330, 780, 1330 and 1600 cm^{-1} [Fig. 5, spectrum (*2*)]. The first two bands are attributable to Ag_n molecular silver clusters with $n < 10$ [35]; the third band, to the Ag_7H^- hydride anion complex [36]; and the fourth and fifth bands, to the Ag_3H^+ hydride cation complex and the Ag_3H neutral hydride complex, respectively [36]. It is also known that molecular silver clusters can form charged and neutral complexes with OH groups, such as $Ag_n(OH)_n$ [37] and $Ag_nO_xH_y$ [38], but their Raman spectra have not yet been studied. Laser irradiation considerably reduces the intensity of all the Raman bands [Fig. 5, spectrum (*3*)]. The decrease in the intensity of the bands related to the molecular silver clusters and their complexes points to a reduction in their concentration as a result of a transformation of the nanoparticles. Silver nanoparticles

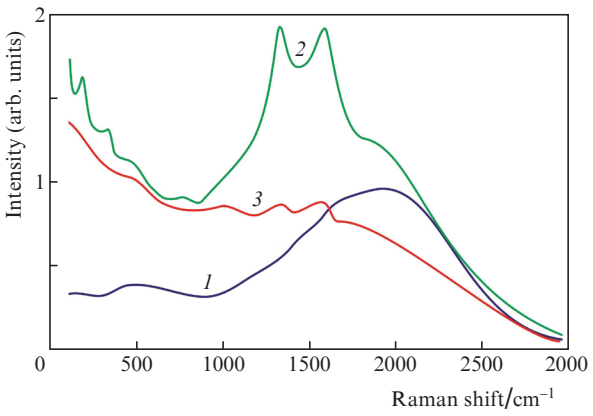

Figure 5. Raman spectra of silver-free NPG (*1*) and silver-containing NPG before (*2*) and after (*3*) laser irradiation; $N = 620$ pulses.

are known to have vibrational bands due to acoustic modes [39, 40], but they lie in the frequency range 20–100 cm^{-1}, which is beyond the working range of the Raman spectrometer used in this study.

The present results demonstrate that the irradiation of silver-containing NPGs with nanosecond laser pulses leads to a transformation of subnanometre molecular silver clusters into silver nanoparticles. The main processes induced by laser irradiation are local heating and photoionisation of the molecular clusters as a result of light absorption. As seen in Fig. 2, the optical density at $\lambda = 532$ nm is 0.8, so both processes have rather high efficiency. Heating and photoionisation lead to fragmentation of some molecular clusters and generation of free electrons and silver ions, which remain in the pores of the NPG. A laser pulse is followed by recombination processes and neutralisation of silver ions. Since this causes Coulomb repulsion to disappear, silver atoms can attach to molecular clusters, increasing their size and improving their stability. This accounts for the increase in optical density in the spectral range 480–700 nm at relatively low laser fluences (less than 50 pulses). At the same time, silver oxide is not formed in the pores because it is thermally unstable. The increase in the size of molecular clusters with increasing laser fluence eventually results in the formation of silver nanoparticles, in which plasmon resonance is possible. Further raising the laser fluence leads to an increase in nanoparticle size and concentration, which is accompanied by an increase in the intensity of the absorption bands in the plasmon resonance region [Fig. 3, curve (*1*)]. At the same time, the concentration of molecular clusters in the irradiated zone decreases. This leads to a reduction in absorption in the spectral range 480–700 nm [Fig. 3, curve (2)]. Since the transverse laser beam profile is bell-shaped, the laser fluence in the peripheral part of the irradiated zone is relatively low. Because of this, there is only an increase in the size of molecular clusters in this region, without formation of silver nanoparticles, which accounts for the presence of a dark ring around the zone under irradiation (Fig. 1). As mentioned above, NPG usually contains adsorbed water monolayers. The photocatalytic decomposition of the water during laser irradiation is accompanied by hydrogen release in the glass pores. This also may contribute to the reduction of silver ions and charged molecular silver clusters after a laser pulse.

Our results can be compared to those reported by Marmugi et al. [19], who observed the formation of potassium nanospheroids in NPG under laser irradiation. It is also worth noting that laser irradiation of monolithic glass containing silver nanoparticles leads to the opposite effect: photodestruction of nanoparticles [10–12].

4. Conclusions

The present results demonstrate that the exposure of NPG containing molecular silver clusters to nanosecond laser pulses leads to the formation of spheroidal silver nanoparticles in the glass pores. This significantly changes the optical properties of the NPG, producing a broad, strong band in the plasmon resonance region, between 350 and 500 nm, in the optical absorption spectrum of the glass. At the same time, the absorption in the spectral range 480–700 nm drops by a factor of 4. Local formation of silver nanoparticles in NPG under laser irradiation can be used for producing chemical and biological sensors, including microfluidic ones, as well as in nonlinear optical and nanoplasmonic devices. The ability to control the optical properties of silver-containing NPGs by laser irradiation can also be used for optical information recording, including digital information in higher order codes.

Acknowledgements. This work was supported by the RF Ministry of Education and Science (Project No. 16.1651. 2017/4.6).

References

1. Kreibig U., Vollmer M. *Optical Properties of Metal Clusters* (Berlin: Springer, 1995).
2. Klimov V., Sharonova A. *Nanoplasmonics* (Singapore: Pan Stanford Publ., 2014).
3. Thomas S., Nair S.K., Jamal A., Al-Harthi S.H., Varma M.R., Anantharaman M.R. *Nanotechnology*, **19**, 075710 (2008).
4. Larsson M.E., Langhammer C., Zoric I., Bengt K. *Science*, **326**, 1091 (2009).
5. Perez D.P. (Ed.) *Silver Nanoparticles* (Croatia: In-Tech, 2010).
6. Hamanaka Y., Nakamura A., Omi S., Del Fatti N., Flitzanis C. *Appl. Phys. Lett*., **75**, 1712 (1999).
7. Kyoung M., Lee M. *Opt. Commun*., **171**, 145 (1999).
8. Li Y., Koshizaki N., Cai W. *Coord. Chem. Rev*., **255**, 357 (2011).
9. Sarkar D.K., Cloutier F., El Khakani M.A. *J. Appl. Phys*., **97**, 084302 (2005).
10. Badr Y., Abd El Wahed M.G., Mahmoud M.A. *Appl. Surf. Sci*., **253**, 2502 (2006).
11. Badr Y., Mahmoud M.A. *Phys. Lett. A*, **370**, 158 (2007).
12. Podlipensky A.V., Grebenev V., Seifert G., Graener H. *J. Lumin*., **109**, 135 (2004) .
13. Ignatiev A.I., Klyukin D.A., Leontieva V.S., Nikonorov N.V., Shakhverdov T.A., Sidorov A.I. *Opt. Mater. Express*, **5**, 1635 (2015).
14. Klyukin D.A., Dubrovin V.D., Pshenova A.S., Putilin S.E., Shakhverdov T.A., Tsypkin A.N., Nikonorov N.V., Sidorov A.I. *Opt. Eng*., **55**, 067101 (2016).
15. Kreisberg V.A., Antropova T.V. *Microporous Mesoporous Mater*., **190**, 128 (2014).
16. Andreeva O.V., Obyknovennaya I.E., Gavrilyuk E.R., Paramonov A.A., Kushnarenko A.P. *J. Opt. Technol*., **72**, 916 (2005).
17. Gutina A., Antropova T., Rysiakiewicz-Pasek E., Virnik K., Feldman Y. *Microporous Mesoporous Mater*., **58**, 237 (2003).
18. Burchianti A., Marinelli C., Mariotti E., Bogi A., Marmugi L., Giomi S., Maccari M., Veronesi S., Moi L. *Quantum Electron*., **44**, 263 (2014) [*Kvantovaya Elektron*., **44**, 263 (2014)].
19. Marmugi L., Mariotti E., Burchianti A., Veronesi S., Moi L., Marinelli C. *Laser Phys. Lett*., **11**, 085902 (2014).
20. Kostyuk G.K., Sergeev M.M., Girsova M.A., Yakovlev E.B., Anfimova I.N., Antropova T.V. *Glass Phys. Chem*., **40**, 415 (2014).
21. Girsova M.A., Drozdova I.A., Antropova T.V. *Glass Phys. Chem*., **40**, 162 (2014).
22. Sergeev M.M., Kostyuk G.K., Zakoldaev R.A., Girsova M.A., Anfimova I.N., Antropova T.V. *Glass Phys. Chem*., **43**, 395 (2017).
23. Antropova T.V., Baran J., Gavrilko T., Gnatyuk I., Morawska-Kowal T., Melnik V., Puchkovska G., Vorobjev V. *Opt. Appl.*, **35**, 725 (2005).
24. Ozin G.A., Huber H. *Inorg. Chem*., **17**, 155 (1978) .
25. Ozin G.A., Hugues F. *J. Phys. Chem*., **87**, 94 (1983).
26. Ozin G.A., Hugues F., Mattar S.M., McIntosh D.F. *J. Phys. Chem*., **87**, 3445 (1983).
27. Félix C., Sieber C., Harbich W., Buttet J., Rabin I., Schulze W., Ertl G. *Chem. Phys. Lett*., **313**, 105 (1999).
28. Fedrigo S., Harbich W., Buttet J. *J. Chem. Phys*., **99**, 5712 (1993).
29. Bohren C.F., Huffman D.R. *Absorption and Scattering of Light by Small Particles* (Weinheim: Wiley-VCH Verlag GmbH, 1998).

30. Irani G.B., Huen T., Woolen F. *J. Opt. Soc. Am*., **61**, 128 (1971).
31. Agamalian M., Drake J.M., Sinha S.K., Axe J.D. *Phys. Rev. E*, **55**, 3021 (1997).
32. Crupi V., Longo F., Majolino D., Venuti V. *Eur. Phys. J.: Spec. Top.*, **141**, 61 (2007).
33. Artlett C.P., Pask H.M. *Opt. Express*, **23**, 31844 (2015).
34. Yakovenko A.A., Yashin V.A., Kovalev A.E., Fesenko E.E. *Biophysics*, **47**, 891 (2002).
35. Bosnick K.A., Haslett T.L., Fedrigo S., Moskovits M., Chan W-T., Fournier R. *J. Chem. Phys*., **111**, 8867 (1999).
36. Zhao S., Liu Z.-P., Li Z.-H., Wang W.-N., Fan K.-N. *J. Phys. Chem. A*, **110**, 11537 (2006).
37. Bertolusa M., Brenner V., Milli P. *Eur. Phys. J. D*, **11**, 387 (2000).
38. Brechignac C., Cahuzac P., Leygnier J., Tigneres I. *Chem. Phys. Lett*., **303**, 304 (1999).
39. Margueritat J., Gonzalo J., Afonco C.N., Bacchelier G., Mlayah A., Laarakker A.S., Murray D.B., Sviot L. *Appl. Phys. A*, **89**, 369 (2007).
40. Kurbatova N.V., Galyautdinov M.F., Shtyrkov E.I., Nuzhdin V.I., Stepanov A.L. *Phys. Solid State*, **52**, 1255 (2010).